# Morphology and Metamorphosis of *Eupsophus calcaratus* Tadpoles (Anura: Leptodactylidae)

**M.F. Vera Candioti,[1]* C. Úbeda,[2] and E.O. Lavilla[1]**

[1]*CONICET and Instituto de Herpetología, Fundación Miguel Lillo, San Miguel de Tucumán, T4000JFE, Argentina*
[2]*Departamento de Zoología, Centro Regional Bariloche, Universidad Nacional del Comahue, San Carlos de Bariloche, R8400FRF, Argentina*

*ABSTRACT* *Eupsophus calcaratus*, a leptodactyloid frog from the austral Andean forests of Argentina and Chile, has endotrophic, nidicolous tadpoles. We studied a metamorphic series from Stages 31 to 46 of Gosner's developmental table (1960). Other than the scarce pigmentation, proportionately large eyes, and massive developing hindlimbs, the remaining external characters are similar to those of generalized, exotrophic larvae. At the same time, internal morphology does not reveal any character state attributable to the endotrophic-nidicolous way of life; conversely, structures such as the hyobranchial skeleton and the mandibular cartilages are similar to those of exotrophic-macrophagous tadpoles. The metamorphic process is characterized by the delayed development of diverse structures (e.g., ethmoid region, palatoquadrate, and hyobranchial apparatus), and the retention of some larval characters (e.g., parietal fenestrae, overall absence of ossification) with the absence of development of some "juvenile" characters (e.g., adult otic process, several bones) in metamorphosed individuals. These heterochronic processes and truncation of larval development are related to a shorter larval life (when compared to other species of the austral Andean region) and to the small size at metamorphosis. J. Morphol. 262:161–177, 2005.


KEY WORDS: *Eupsophus calcaratus*; endotrophic nidicolous tadpoles; morphology; metamorphosis

*Eupsophus calcaratus*, a leptodactyloid frog from the austral Andean forests of Argentina and Chile, has endotroph-nidicolous tadpoles. Such tadpoles are free-living larvae that do not feed actively, but obtain their nutrients from the vitellum (Altig and Johnston, 1989). The only available information regarding these larvae is that of Formas (1989), who described their larval external morphology at Gosner's (1960) Stage 37, but nothing is known regarding internal morphology and/or ontogeny.

The aim of the present contribution is to provide a comprehensive description of external morphology, the chondrocranium and hyobranchial apparatus, musculature, and metamorphosis of *Eupsophus calcaratus* tadpoles, analyzing structural features in the context of their endotrophic development.

## MATERIALS AND METHODS

A sample of 48 larvae of *Eupsophus calcaratus* was collected in a forest at the northern margin of Lago Paimún (Lanín National Park, Neuquén, Argentina) during January, 1997. Some specimens were immediately preserved (Stage 31, Gosner, 1960), and the remaining were kept in captivity, preserving a sample each time an ontogenetic change was observed. The material was fixed with 10% formalin and cleared and stained following Wassersug's (1976) protocol. The muscles were contrasted with a lugol solution (Bock and Shear, 1972).

For the analysis, larvae were grouped in five periods following Fabrezi's (1988) proposal: Stages 31–36 (Period V), Stages 37–41 (Period VI), Stage 42 (Period VII), Stages 43–45 (Period VIII), and Stage 46 (Period IX). Morphology was thoroughly described only for the first period; in those subsequent, only changes were indicated. Measurements are shown in Table 1.

Internal morphology terminology follows that of Cannatella (1999). The studied material is housed in the Herpetological Collection of Fundación Miguel Lillo (FML 15859) (see Appendix).

## RESULTS

### Stages 31–36

**External morphology (Fig. 1).** At the beginning of the period the skin is smooth and transparent, with progressively visible chromatophores, and two longitudinal bands between dorsal musculature and vitellum are defined at Stage 34; the ventral region, tail, and caudal fins remain unpigmented. The orbitonasal line, slightly pigmented, is visible at the end of the period. The body is elliptical, twice as long as high, and slightly depressed. It represents one-third of the total length and the maximum width is at the posterior third. The body contour shows a slight constriction at each side between head and trunk, whereas the

Contract grant sponsor: CONICET; Contract grant number: PIP 02668; Contract grant sponsor: Universidad Nacional del Comahue (B 101), Argentina.

*Correspondence to: María Florencia Vera Candioti, Instituto de Herpetología, Fundación Miguel Lillo, Miguel Lillo 251, San Miguel de Tucumán, T4000JFE, Argentina.
E-mail: florivc@hotmail.com

Published online 10 March 2005 in
Wiley InterScience (www.interscience.wiley.com)
DOI: 10.1002/jmor.10320

*TABLE 1. Mean ± standard deviation (s) of measurements and ratios of* Eupsophus calcaratus

| Stages | 31–36 | 37–41 | 42 | 43–45 |
|---|---|---|---|---|
| N | 16 | 16 | 4 | 7 |
| Total length | 21.54 ± 1.79 | 23.41 ± 0.88 | 23.39 ± 0.95 | 14.17 ± 3.28 |
| Snout–vent length | 6.85 ± 0.41 | 7.51 ± 0.25 | 7.65 ± 0.13 | 8.04 ± 0.41 |
| Tail length | 14.64 ± 1.59 | 15.90 ± 0.73 | 15.74 ± 0.93 | 6.13 ± 3.04 |
| Maximum body height | 3.51 ± 0.28 | 3.53 ± 0.18 | 3.30 ± 0.16 | 3.24 ± 0.40 |
| Maximum tail height | 4.17 ± 0.65 | 4.61 ± 0.22 | 4.13 ± 0.46 | 1.77 ± 0.61 |
| Caudal musculature height (at the base) | 1.65 ± 0.2 | 1.87 ± 0.11 | 1.90 ± 0.08 | 1.89 ± 1.82 |
| Maximum body width | 3.88 ± 0.32 | 4.03 ± 0.19 | 3.60 ± 0.28 | 3.57 ± 0.11 |
| Eye diameter | 0.97 ± 0.08 | 1.10 ± 0.07 | 1.16 ± 0.06 | 1.15 ± 0.09 |
| Interorbital distance | 1.10 ± 0.07 | 1.10 ± 0.09 | 1.11 ± 0.08 | 1.18 ± 0.06 |
| Extraorbital distance | 2.71 ± 0.24 | 3.13 ± 0.25 | 3.04 ± 0.16 | 3.05 ± 0.17 |
| Body width (eye level) | 3.15 ± 0.30 | 3.57 ± 0.18 | 3.53 ± 0.17 | 3.14 ± 0.29 |
| Nostril diameter | 0.15 ± 0.04 | 0.18 ± 0.06 | 0.24 ± 0.03 | 0.21 ± 0.04 |
| Internarial distance | 0.99 ± 0.06 | 0.97 ± 0.10 | 0.94 ± 0.07 | 0.98 ± 0.05 |
| Extranarial distance | 1.36 ± 0.11 | 1.40 ± 0.21 | 1.32 ± 0.07 | 1.26 ± 0.07 |
| Body width (nostril level) | 2.05 ± 0.27 | 2.11 ± 0.24 | 2.00 ± 0.23 | 1.59 ± 0.26 |
| Rostronasal distance | 0.48 ± 0.10 | 0.34 ± 0.08 | 0.31 ± 0.04 | 0.26 ± 0.09 |
| Orbitonasal distance | 0.59 ± 0.07 | 0.68 ± 0.07 | 0.65 ± 0.07 | 0.65 ± 0.03 |
| Rostro-ocular distance | 1.20 ± 0.08 | 1.18 ± 0.10 | 1.11 ± 0.08 | 1.11 ± 0.17 |
| Rostro-spiracular distance | 3.98 ± 0.31 | 4.08 ± 0.16 | 3.63 ± 0.29 | 3.20 |
| Vent tube length | 1.50 ± 0.17 | 1.25 ± 0.15 | | |
| Vent tube width | 0.7 ± 0.10 | 0.58 ± 0.06 | | |
| Limb length | 2.89 ± 0.85 | 6.44 ± 0.99 | 7.90 ± 0.26 | 9.54 ± 0.32 |
| Oral disc width | 1.50 ± 0.19 | 1.60 ± 0.08 | 1.63 ± 0.10 | |
| Rostral gap width | 0.75 ± 0.15 | 0.71 ± 0.10 | 0.70 ± 0.05 | |
| Suprarostrodont length | 0.56 ± 0.07 | 0.60 ± 0.09 | | |
| Infrarostrodont length | 0.46 ± 0.05 | 0.44 ± 0.06 | | |
| Snout–vent length/Total length | 0.32 ± 0.02 | 0.32 ± 0.01 | 0.33 ± 0.01 | 0.59 ± 0.13 |
| Maximum body width/Maximum body height | 1.11 ± 0.07 | 1.14 ± 0.04 | 1.09 ± 0.10 | 1.11 ± 0.13 |
| Rostronasal distance/Rostro-ocular distance | 0.40 ± 0.09 | 0.28 ± 0.06 | 0.28 ± 0.02 | 0.23 ± 0.07 |
| Rostro-spiracular distance/Snout–vent length | 0.58 ± 0.03 | 0.54 ± 0.03 | 0.47 ± 0.04 | 0.40 |
| Snout–vent length/Maximum body height | 1.96 ± 0.14 | 2.13 ± 0.12 | 2.32 ± 0.10 | 2.50 ± 0.23 |
| Tail length/Maximum body height | 1.19 ± 0.18 | 1.31 ± 0.06 | 1.26 ± 0.20 | 0.52 ± 0.15 |
| Caudal musculature height/Maximum body height | 0.47 ± 0.07 | 0.53 ± 0.04 | 0.58 ± 0.00 | 0.65 ± 0.77 |
| Extranarial distance/Body width (nostril level) | 0.66 ± 0.12 | 0.68 ± 0.22 | 0.66 ± 0.07 | 0.81 ± 0.16 |
| Rostronasal distance/Orbitonasal distance | 0.80 ± 0.19 | 0.50 ± 0.14 | 0.48 ± 0.03 | 0.39 ± 0.13 |
| Internarial distance/Interorbital distance | 0.91 ± 0.06 | 0.89 ± 0.12 | 0.84 ± 0.07 | 0.82 ± 0.04 |
| Interorbital distance/Maximum body width | 0.28 ± 0.02 | 0.27 ± 0.02 | 0.31 ± 0.01 | 0.33 ± 0.02 |
| Eye diameter/Body width (eye level) | 0.31 ± 0.03 | 0.31 ± 0.02 | 0.33 ± 0.02 | 0.37 ± 0.04 |
| Interorbital distance/Eye diameter | 1.14 ± 0.07 | 1.00 ± 0.09 | 0.96 ± 0.06 | 1.03 ± 0.12 |
| Extraorbital distance/Body width (eye level) | 0.86 ± 0.08 | 0.88 ± 0.09 | 0.86 ± 0.05 | 0.97 ± 0.06 |
| Oral disc width/Maximum body width | 0.39 ± 0.03 | 0.40 ± 0.03 | 0.45 ± 0.05 | |
| Rostral gap width/Oral disc width | 0.50 ± 0.06 | 0.44 ± 0.06 | 0.43 ± 0.01 | |
| Suprarostrodont length/Infrarostrodont length | 1.23 ± 0.16 | 1.30 ± 0.16 | | |
| Vent tube length/Snout–vent length | 0.22 ± 0.03 | 0.17 ± 0.02 | | |

Measurements expressed in mm. Stages according to Gosner (1960).

ventral outline is convex. In dorsal view the snout is rounded, with oval, small, protruded, and dorsolateral nares, without projections or inflections. The eyes are large, lateral, and anterodorsolaterally oriented; the iris, defined at Stage 35, has an umbraculum and ventral notch; the lower eyelids are insinuated. The spiracular tube is single, sinistral and ventral, and has a visible opening. The development of the anterior limbs, in the opercular chambers, starts at Stage 33 and by the end of the period the hands have four digits formed. The vitellum is abundant and occupies most of the abdominal cavity. The proctodeal tube and its opening are medial; the tube is slightly wider in the central portion. The caudal musculature is moderately robust, with 23–27 myotomes and a straight axis. Fins have equal development, with maximum height at half of their length. The dorsal fin starts on the posterior third of the body and has a slightly curved margin; the ventral one starts posteriorly to the proctodeal tube and has a nearly straight inferior margin.

The oral disc is subterminal and ventral, with lateral constrictions. The margin bears a single row of low and rounded papillae, interrupted by a rostral gap. The rostrodonts, well keratinized and pigmented, are wider than high and have acute serrations. Keratodonts are small and numerous (32–42 keratodonts/mm), and generally grouped according to the formula 1(1-1)/2; a few individuals had 1(1-1)/

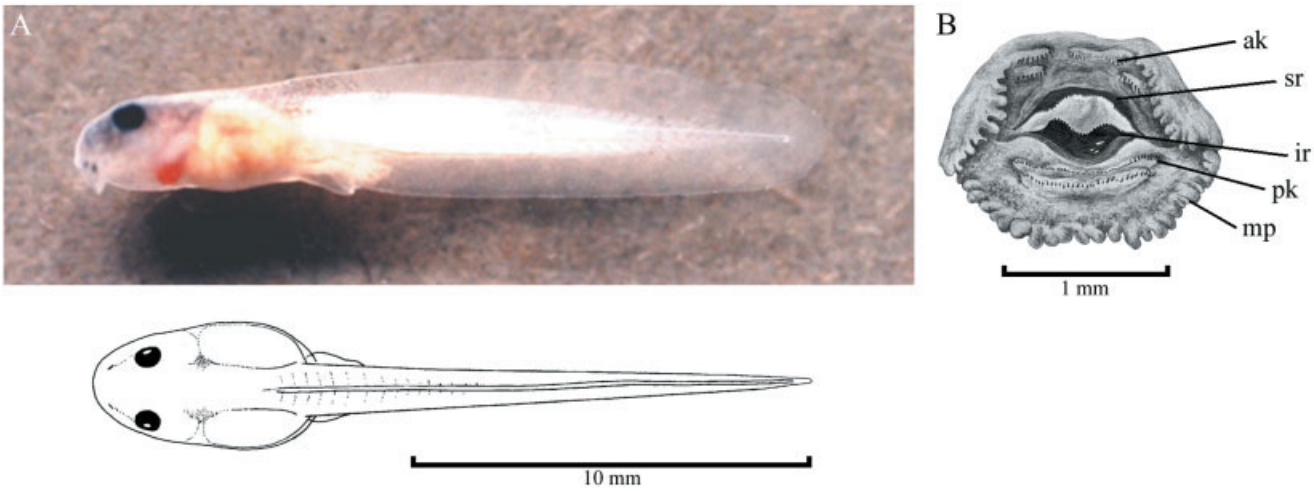


Fig. 1. *Eupsophus calcaratus* Stage 35. **A:** Tadpole, lateral and dorsal views. **B:** Oral disc, ventral view. ak, anterior keratodonts; ir, infrarostrodont; mp, marginal papillae; pk, posterior keratodonts; sr, suprarostrodont.

1(1-1) and one, at Stage 36, had a vestigial third lower labial ridge. The reduction of the keratinized pieces starts at the end of the period, a few, isolated keratodonts remaining.

**Skeleton (Fig. 2).** The suprarostral corpus is single, strongly chondrified, and with a deep notch in the mid-dorsal region. The alae are subtriangular, with a long and blunt processus dorsalis posterior; they join the corpus by a cartilaginous dorsal commissure. Corpus and alae are obliquely located regarding the axial axis, and are syndesmotically attached to the trabecular horns.

The trabecular horns are short (10.5% of the chondrocranium length). Wider at the base, they bend downwards and outwards, diverging regularly. The ethmoid plate is separated from the trabecular horns by a thin cartilaginous sheet, corresponding to the mid-portion of the orbitonasal plate.

The orbital cartilages, less chondrified, are subtriangular and bear well-developed optic and oculomotor foramina; the first foramen is 2.25 times larger that the second one. The trochlear foramen, less well defined, is smaller and placed above the optic and oculomotor foramina. The taenia tecti marginalis does not reach the otic capsule, so the prootic foramina are open dorsally.

The floor of the cranial cavity is weakly chondrified; the basicranial fenestra is occluded and the craniopalatine and carotid foramina are poorly defined. The notochord penetrates about one-third the length of the cranial cavity floor.

The occipital arch is thin and fused to the internal walls of the otic capsules; the jugular foramina are well defined, and the occipital condyles are present as small protuberances. The otic capsules correspond to 37% of the total length of the neurocranium. The oval fenestra corresponds to about half the length of the otic capsule. The operculum, crista parotica, and larval otic process are not defined, whereas the acoustic, endolymphatic, and perilymphatic foramina are evident.

The ascending process of the palatoquadrate, relatively thin and strongly chondrified, fuses to the pila antotica above the oculomotor foramen. The subocular bar is laminar; some individuals bear a conspicuous foramen of unknown homology at the posterior region.

The muscular process is wide, subtriangular, strongly chondrified, and vertically disposed. The quadratocranial commissure has a small quadratoethmoid process on the anterior margin, but no pseudopterygoid process is present posteriorly. The muscular funnel is open dorsally.

Meckel's cartilage is twisted and has a blunt retroarticular process; the proximal region is wider than the distal, and is joined to the infrarostral via a short, nonchondrified, intermandibular commissure. The infrarostral cartilages, curved posteriorly and wider in the external margin, are joined in a single structure through a cartilaginous intramandibular commissure.

In the hyobranchial apparatus the ceratohyals are the most chondrified structures; the articular condyle is short and the processus anterior hyalis and lateralis are triangular. Copula I is absent. The pars reuniens, copula II, and hypobranchial plates form a continuous, scarcely chondrified structure, posteriorly notched. A very small, rounded, urobranchial process is present in the region corresponding to copula II. The branchial basket is composed of four ceratobranchials with no lateral projections; the scarcely chondrified terminal commissures are present, as are four weak spicules, spicule IV being almost vestigial.

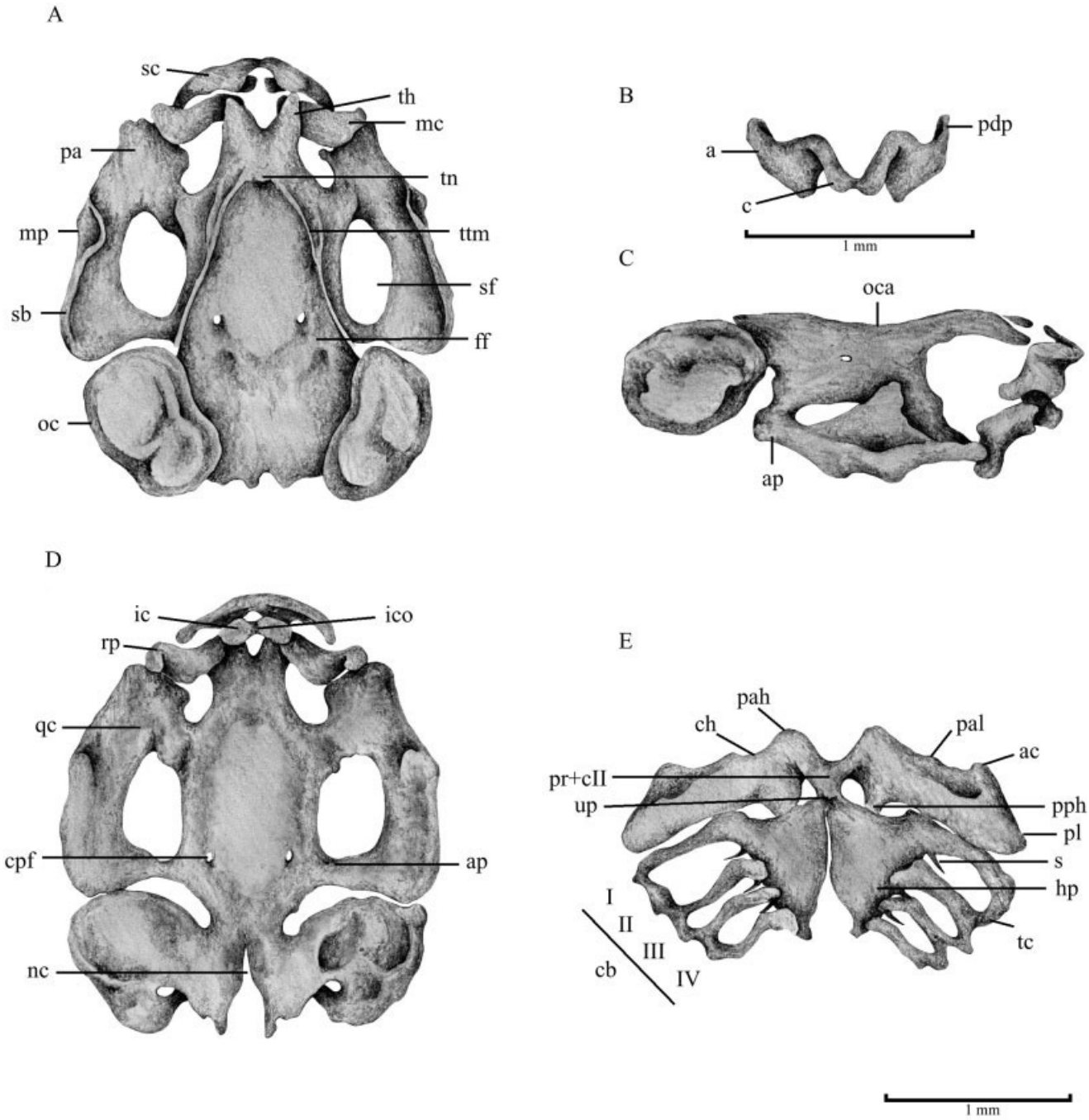


Fig. 2. *Eupsophus calcaratus* Stage 31. Chondrocranium and visceral skeleton. **A:** Chondrocranium, dorsal view. **B:** Suprarostral cartilage, frontal view. **C:** Chondrocranium, lateral view. **D:** Chondrocranium, ventral view. **E:** Hyobranchial skeleton, ventral view. a, ala; ac, articular condyle; ap, ascending process; c, corpus; cb (I-IV), ceratobranchials; ch, ceratohyal; cII, copula II; cpf, craniopalatine foramen; ff, frontoparietal fenestra; hp, hypobranchial plate; ic, infrarostral cartilage; ico, intramandibular commissure; mc, Meckel's cartilage; mp, muscular process; nc, notochordal canal; oc, otic capsule; oca, orbital cartilage; pa, pars articularis; pah, processus anterior hyalis; pal, processus anterolateralis; pdp, processus dorsalis posterior; pl, processus lateralis; pph, processus posterior hyalis; pr, pars reuniens; qc, quadratocranial commissure; rp, retroarticular process; s, spicule; sb, subocular bar; sc, suprarostral cartilage; sf, subocular fenestra; tc, terminal commissure; th, trabecular horn; tn, tectum nasi; ttm, taenia tecti marginalis; up, urobranchial process.

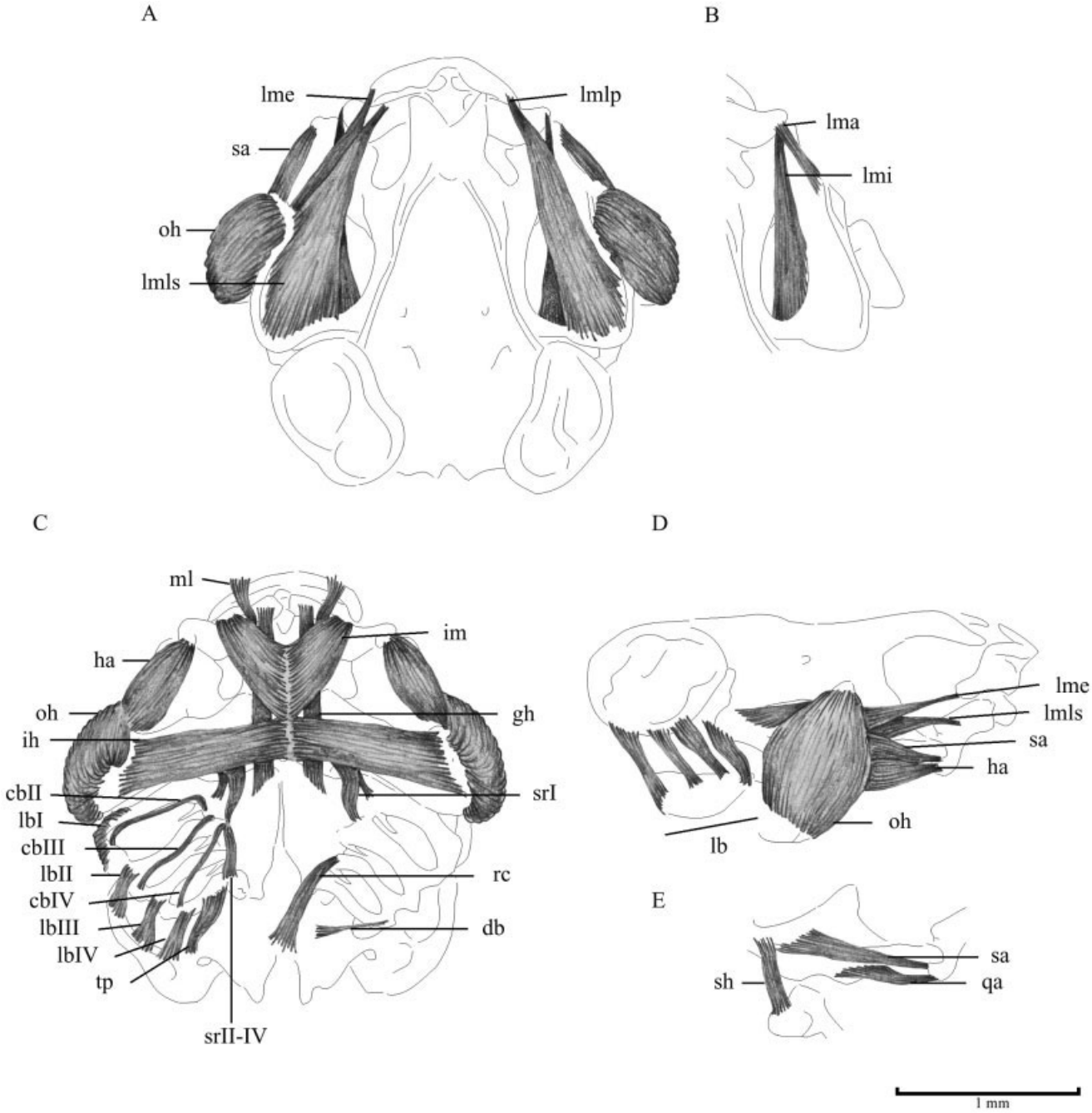


Fig. 3. *Eupsophus calcaratus* Stage 31. Musculature. **A:** Dorsal view, superficial plane. **B:** Dorsal view, deep plane. **C:** Ventral view. **D:** Lateral view, superficial plane. **E:** Lateral view, deep plane. cb (II-IV), *constrictor branchialis*; db, *diaphragmatobranchialis*; gh, *geniohyoideus*; ha, *hyoangularis*; ih, *interhyoideus*; im, i*ntermandibularis*; lb (I-IV), *levator arcus branchialium*; lma, *levator mandibulae articularis*; lme, *levator mandibulae externus*; lmi, *levator mandibulae internus*; lmlp, *levator mandibulae longus profundus*; lmls, *levator mandibulae longus superficialis*; ml, *mandibulolabialis*; oh, *orbitohyoideus*; qa, *quadratoangularis*; rc, *rectus cervicis*; sa, *suspensorioangularis*; sh, *suspensoriohyoideus;* srI, *subarcualis rectus I*; srII-IV, *subarcualis rectus II-IV*; tp, *tympanopharyngeus*.

**Musculature (Fig. 3).** The configuration of the muscles in this period is summarized in Table 2.

### Stages 37–41

**External morphology.** The skin of dorsum and limbs becomes finely granular, with an intensification of the dorsal coloration, especially on the scapular region. The abdomen and hindlimbs are slightly pigmented, whereas the tail and fins show only scattered chromatophores. The snout is slightly truncated. The upper eyelid begins its development. The spiracular opening enlarges at the end of the period,

*TABLE 2. Musculature of* Eupsophus calcaratus, *Stages 31–36*

| Muscle | Origin | Insertion | Comments |
|---|---|---|---|
| *M. mandibulolabialis* | ventromedial surface of Meckel's cartilage | lower lip of the oral disc | single slip |
| *M. intermandibularis* | middle region of Meckel's cartilage | medial aponeurosis | triangular shape, joined to the *M. interhyoideus* aponeurosis |
| *M. levator mandibulae longus superficialis* | external border of subocular bar and ascending process | medial extreme of Meckel's cartilage | conceals almost completely the subocular fenestra |
| *M. levator mandibulae longus profundus* | external border of subocular bar and ascending process | ala of suprarostral cartilage | |
| *M. levator mandibulae internus* | ventral surface of ascending process | distal extreme of Meckel's cartilage | |
| *M. levator mandibulae externus* | medial inferior surface of muscular process | ala of suprarostral cartilage | inserts via a long tendon shared with *M. l.m.l. profundus* |
| *M. levator mandibulae articularis* | medial inferior surface of muscular process | Meckel's cartilage | runs ventrally regarding *M. l.m. externus* |
| *M. suspensoriohyoideus* | external descending border of muscular process | posterior face of the extreme of ceratohyal | |
| *M. orbitohyoideus* | external anterior and superior borders of muscular process | extreme of ceratohyal | covers *M. suspensoriohyoideus* |
| *M. suspensorioangularis* | external posterior surface of muscular process | retroarticular process of Meckel's cartilage | |
| *M. quadratoangularis* | ventral surface of palatoquadrate | retroarticular process of Meckel's cartilage | concealed by *Mm. suspensorioangularis* and *hyoangularis* |
| *M. hyoangularis* | dorsal face of ceratohyal | retroarticular process of Meckel's cartilage | |
| *M. interhyoideus* | ventral face of the extreme of ceratohyal | medial aponeurosis | formed by transverse, parallel fibers |
| *M. geniohyoideus* | ventral face of infrarostrals | hypobranchial plate | short, flat muscle |
| *M. levator arcus branchialium I* | lateral margin of subocular bar | ceratobranchial I | |
| *M. levator arcus branchialium II* | otic capsule | terminal commissure I | |
| *M. levator arcus branchialium III* | lateral region of otic capsule | terminal commissure II | |
| *M. levator arcus branchialium IV* | posterolateral region of otic capsule | terminal commissure III | |
| *M. constrictor branchialis II* | proximal extreme of ceratobranchial II | terminal commissure I | |
| *M. constrictor branchialis III* | proximal extreme of ceratobranchial II | terminal commissure II | |
| *M. constrictor branchialis IV* | proximal extreme of ceratobranchial III | terminal commissure III | |
| *M. subarcualis rectus I* | lateral region of processus posterior hyalis | proximal end of ceratobranchial II and proximal extreme of ceratobranchial I | ventral and dorsal heads |
| *M. subarcualis rectus II–IV* | ventromedial face of ceratobranchial IV | proximal end of the ceratobranchial II | |
| *M. tympanopharyngeus* | ceratobranchial IV | otic capsule | |
| *M. diaphragmato-branchialis* | peritoneum | distal end of ceratobranchial IV | |
| *M. rectus cervicis* | peritoneum | distal end of ceratobranchial II | |

and the orifice through which the right forelimb will emerge is defined. The foot bears the first traces of subarticular and inner and outer metatarsal tubercles. The regression of the proctodeal tube begins. In the oral disc, rostrodonts and keratodonts disappear at Stage 38. Toward Stage 41, the buccal opening is insinuated under the skin.

**Skeleton (Fig. 4).** The chondrocranium grows in length and width. The suprarostral alae disappear and the corpus loses the cartilaginous commissure. The infrarostrals and Meckel's cartilage extend transversely. The ventromedial processes of Meckel's cartilage become less obvious. The trabecular horns are slightly shortened. In the ethmoid region, the antorbital process enlarges and is oriented anterolaterally. The pseudopterygoid process develops on the quadratocranial commissure. The otic capsules increase in size and the tectum synoticum is chondrified. The taeniae tecti transversalis and medialis are evident. In the hyobranchial skeleton, the terminal commissures begin to disappear. The hyoglossal sinus becomes deeper.

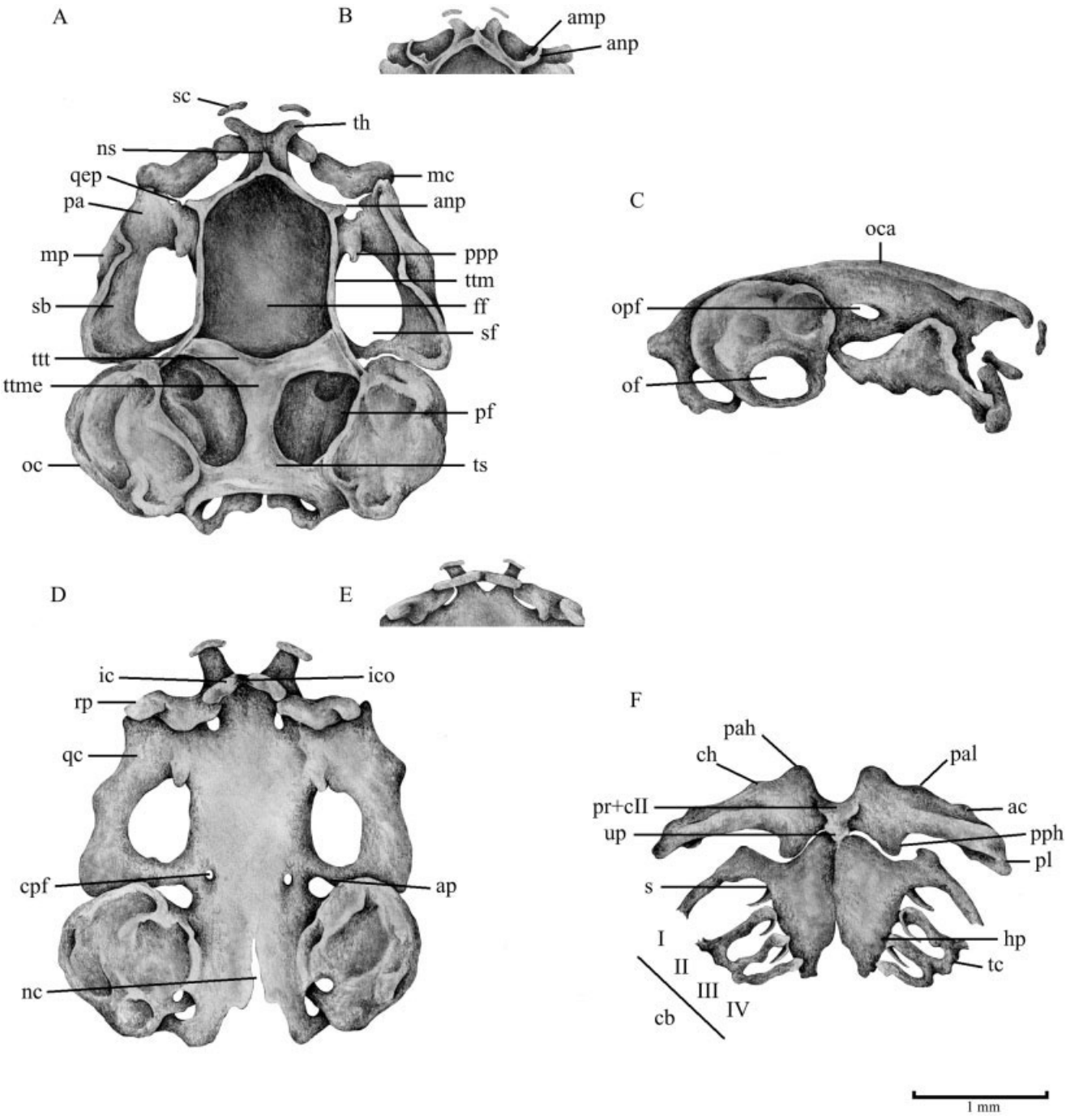


Fig. 4. *Eupsophus calcaratus* Stage 39. Chondrocranium and visceral skeleton. **A:** Chondrocranium, dorsal view. **B:** Detail of ethmoid region, Stage 42–43. **C:** Chondrocranium, lateral view. **D:** Chondrocranium, ventral view. **E:** Detail of ethmoid region, Stage 42–43. **F:** Hyobranchial skeleton, ventral view. ac, articular condyle; amp, anterior maxillary process; anp, antorbital process; ap, ascending process; cb (I-IV), ceratobranchials; ch, ceratohyal; cII, copula II; cpf, craniopalatine foramen; ff, frontoparietal fenestra; hp, hypobranchial plate; ic, infrarostral cartilage; ico, intramandibular commissure; mc, Meckel's cartilage; mp, muscular process; nc, notochordal canal; ns, nasal septum; oc, otic capsule; oca, orbital cartilage; of, oval fenestra; opf, optic foramen; pa, pars articularis; pah, processus anterior hyalis; pal, processus anterolateralis; pf, parietal fenestra; pl, processus lateralis; pph, processus posterior hyalis; ppp, pseudopterygoid process; pr, pars reuniens; qc, quadratocranial commissure; qep, quadratoethmoid process; rp, retroarticular process; s, spicule; sb, subocular bar; sc, suprarostral cartilage; sf, subocular fenestra; tc, terminal commissure; th, trabecular horn; ttm, taenia tecti marginalis; ttme, taenia tecti medialis; ttt, taenia tecti transversalis; ts, tectum synoticum; up, urobranchial process.

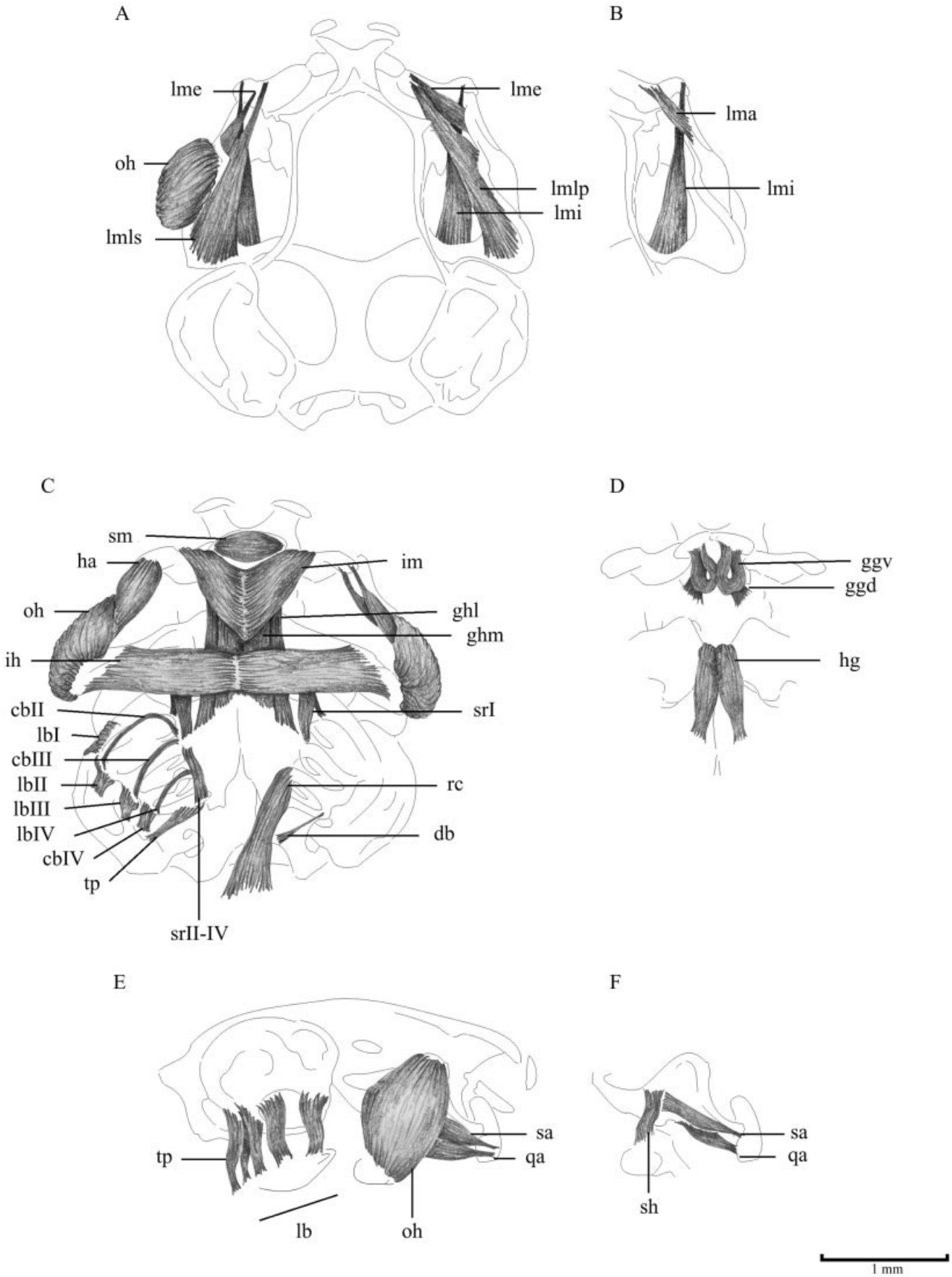
A
lme
lme
oh
lmlp
lmi
lmls
B
lma
lmi
C
sm
ha
im
oh
ghl
ghm
ih
cbII
srI
lbI
cbIII
lbII
rc
lbIII
lbIV
db
cbIV
tp
srII-IV
D
ggv
ggd
hg
E
tp
sa
qa
lb
oh
F
sa
qa
sh
1 mm

Figure 5

**Musculature (Fig. 5).** The *M. mandibulolabialis* disappears. The *M. intermandibularis* frees from the aponeurosis of the *M. interhyoideus*. The *M. l. m. longus profundus* changes its insertion to Meckel's cartilage, due to the changes in the suprarostral cartilage. The *M. geniohyoideus* divides into *M. geniohyoideus medialis*, which inserts on connective tissue between ceratohyals and the hypobranchial plate, and the *M. geniohyoideus lateralis*, inserted on the hypobranchial plate-ceratobranchial II junction. Three new muscles differentiate: the *M. submentalis*, which extends between the ventromedial regions of infrarostral cartilages; the *M. hyoglossus*, originating on the hypobranchial plate, at the same level as the *M. geniohyoideus medialis*, and inserting in the tongue anlage; and the *M. genioglossus*, which originates on the ventral face of the infrarostral and inserts in the tongue anlage.

### Stage 42

**External morphology.** The forelimbs are externally visible. The patterns of dorsum and limb coloration insinuate, while the abdomen and tail are scarcely pigmented; the fins remain unpigmented. The eyes are slightly protruded and oriented anterolaterally. The eyelids are still developing. The limbs bear metacarpal, metatarsal, and rounded subarticular tubercles. The origin of the dorsal fin draws back to the body/tail junction; fins are lower than in previous stages. The buccal commissure, visible under the skin but still not open, is placed between the nostril and the anterior margin of the eye.

**Skeleton (Fig. 4).** The infrarostrals grow longer and fuse, forming a slightly curved, transversely oriented structure. The retroarticular process of Meckel's cartilage is less evident. The trabecular horns are reduced in length by 50%. The antorbital processes lengthen and curve anteriorly and the anterior maxillary process begins its development.

**Musculature.** The *Mm. suspensoriohyoideus* and *orbitohyoideus* fuse, and the *Mm. tympanopharyngeus* and *diaphragmatobranchialis* disappear.

Fig. 5. *Eupsophus calcaratus* Stage 39. Musculature. **A:** Dorsal view, superficial plane. **B:** Dorsal view, deep plane. **C:** Ventral view, superficial plane. **D:** Ventral view, deep plane. **E:** Lateral view, superficial plane. **F:** Lateral view, deep plane. cb (II-IV), *constrictor branchialis*; db, *diaphragmatobranchialis*; ggd, *genioglossus dorsalis*; ggv, *genioglossus ventralis*; ghl, *geniohyoideus lateralis*; ghm, *geniohyoideus medialis*; ha, *hyoangularis*; hg, *hyoglossus*; ih, *interhyoideus*; im, *intermandibularis*; lb (I-IV), *levator arcus branchialium*; lma, *levator mandibulae articularis*; lme, *levator mandibulae externus*; lmi, *levator mandibulae internus*; lmlp, *levator mandibulae longus profundus*; lmls, *levator mandibulae longus superficialis*; oh, *orbitohyoideus*; qa, *quadratoangularis*; rc, *rectus cervicis*; sa, *suspensorioangularis*; sh, *suspensoriohyoideus*; sm, *submentalis*; srI, *subarcualis rectus I*; srII-IV, *subarcualis rectus II-IV*; tp, *tympanopharyngeus*.

### Stages 43–45

**External morphology.** The skin becomes more verrucose, and some fringes on head and limbs are evident. The definitive adult coloration is achieved at Stage 45. The acuminate snout protrudes over the lower jaw. The canthus rostralis is defined. The eyes protrude laterally and the eyelids are completely formed. Large amounts of vitellum remain in the gut. The skin around the armpits starts to fuse at Stage 44. Fingers and toes show thin tips and all the adult tubercles. The tail decreases, remaining as a triangular stub at the end of the period. The mouth is defined and the tongue is present.

**Skeleton (Fig. 6).** The suprarostral cartilages have disappeared. The trabecular horns reorganize, retaining the superior prenasal cartilages and the crista subnasalis. The tectum nasi is well chondrified and the nasal septum is conspicuous and acute. The oblique cartilages have formed, joining posteriorly with the lamina inferior of the antorbital process. The alary and inferior prenasal cartilages appear anteriorly. The anterior and posterior maxillary processes project from the antorbital plate. The former is small and rounded, whereas the latter is very long and joins the quadratoethmoid process, constituting the pterygoid process. The primordia of three dermal bones, still not calcified, appear: the septomaxilla, small and curved; the premaxilla (with the conspicuous palatine processes) attached to the internal surface of the inferior prenasal cartilages; and the maxilla, extending approximately to the half length of the pterygoid process. In the lower jaw the infrarostrals and Meckel's cartilage fuse and the primordia of the dentary and angulosplenial appear. The optic (confluent with the craniopalatine), oculomotor (including carotid), and the prootic foramina are evident in the floor of the cranial cavity. The palatoquadrate is placed vertically; the posterior region of the subocular bar degenerates, losing the connection with the neurocranium. The pars articularis, quadratocranial commissure, and muscular process are not recognizable. The primordium of the squamosal appears as two portions: a vertical element, curved backwards (corresponding to the ventral and zygomatic rami), and a horizontal one, related to the otic capsule (the otic ramus). The oval fenestra bears the operculum. The hyobranchial apparatus has the adult aspect. The ceratohyals, thinner and sigmoid, grow longer and form the hyale; the processus anterior hyalis, posterior hyalis, and lateralis disappear and the articular condyle is reduced. A new cartilaginous piece forms the anterior process of the hyale on the anterior margin. The copula II loses the urobranchial process and fuses to the hypobranchial plates, resulting in the hyoid plate. Posterolateral and posteromedial processes are visible, the latter resulting from the fusion of spicule IV and the posterior portion of the

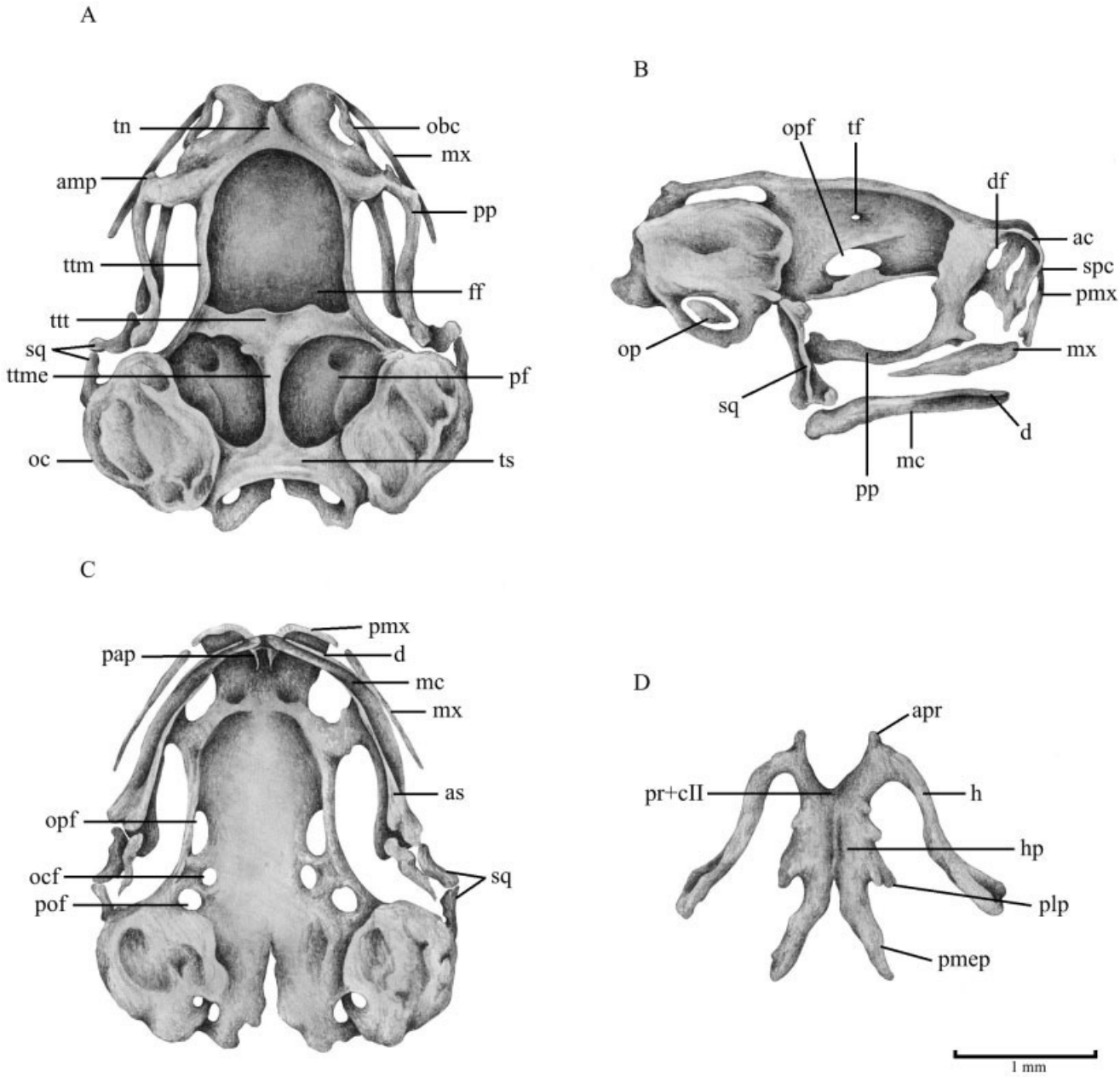


Fig. 6. *Eupsophus calcaratus* Stage 44. Skeleton. **A:** Chondrocranium, dorsal view. **B:** Chondrocranium, lateral view. **C:** Chondrocranium, ventral view. **D:** Hyobranchial skeleton, ventral view. ac, alary cartilage; amp, anterior maxillary process; apr, anterior process; as, angulosplenial; cII, copula II; d, dentary; df, dorsal fenestra; ff, frontoparietal fenestra; h, hyale; hp, hyoid plate; mc, Meckel's cartilage; mx, maxilla; obc, oblique cartilage; oc, otic capsule; ocf, oculomotor foramen; op, operculum; opf, optic foramen; pap, palatine process; pf, parietal fenestra; pmx, premaxilla; plp, posterolateral process; pmep, posteromedial process; pof, prootic foramen; pp, pterygoid process; pr, pars reuniens; spc, superior prenasal cartilage; sq, squamosal; tf, trochlear foramen; tn, tectum nasi; ttm, taenia tecti marginalis; ttme, taenia tecti medialis; ttt, taenia tecti transversalis; ts, tectum synoticum.

hypobranchial plate. Finally, the four ceratobranchials disappear.

**Musculature (Fig. 7).** The *M. intermandibularis* grows and its fibers dispose in two slips, the anterior, with oblique fibers, and the posterior, more developed and transversely placed. The posterior slip forms a band that conceals the anterior region of the hyobranchial apparatus and inserts on the ventromedial face of the angulosplenial primordium. The muscles of the levator complex of the jaw acquire a dorsoventral disposition. The *Mm. levator mandibulae longus superficialis* and *profundus* are joined in a single muscle, the *M. l. m. longus*, which originates on the anterodorsal face of the otic capsule, descends dorsoventrally, and inserts on the internal face of the posterior end of the lower jaw.

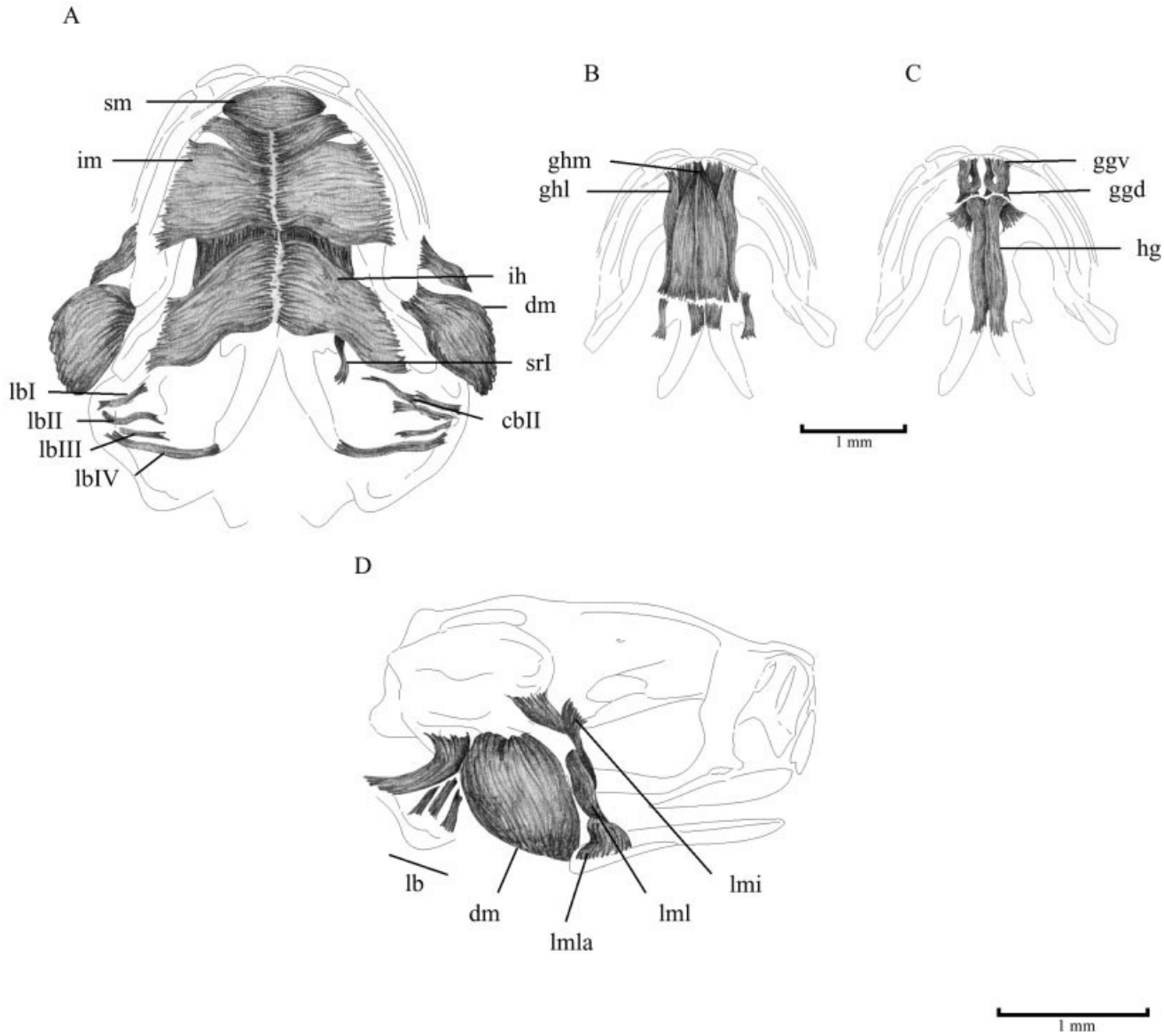


Fig. 7. *Eupsophus calcaratus* Stage 44. Musculature. **A:** Ventral view, superficial plane. **B:** Ventral view, middle plane. **C:** Ventral view, deep plane. **D:** Lateral view. cbII, *constrictor branchialis II*; dm, *depressor mandibulae*; ggd, *genioglossus dorsalis*; ggv, *genioglossus ventralis*; ghl, *geniohyoideus lateralis*; ghm, *geniohyoideus medialis*; hg, *hyoglossus*; ih, *interhyoideus*; im, *intermandibularis*; lb (I-IV), *levator arcus branchialium*; lmi, *levator mandibulae internus*; lml, *levator mandibulae longus*; lmla, *levator mandibulae lateralis*; sm, *submentalis*; srI, *subarcualis rectus I*.

The *M. l. m. internus* changes its origin to the anterodorsal face of the otic capsule (medial and anterior with respect to the *M. l. m. longus*), and inserts on the inner face of the lower jaw. The *M. l. m. externus* extends between the primordium of the zygomatic ramus of the squamosal and the dorsal margin of the rear end of the lower jaw (medial with regard to the *M. l. m. longus*). The *M. l. m. articularis* is the most superficial; this muscle originates on the ventral ramus of the squamosal and inserts on the dorsal surface of the lower jaw. Finally, the *M. l. m. lateralis* arises, with fibers originating on a small, external and anterior surface of the quadrate, and passing to the external and posterior surface of the lower jaw.

Regarding hyoid and spinal muscles, the *M. interhyoideus* parallels the development of the hyale. The *Mm. quadratoangularis, suspensorioangularis* and *hyoangularis* are fused, composing a single, cylindrical slip that runs from the ventral edge of the otic ramus of the squamosal, to the posterior angle of the lower jaw. The *suspensoriohyoideus–orbitohyoideus* union, located lateral to the former muscles, is placed among the otic ramus of the squamosal, the lateral surface of the otic capsule, and the posterior angle of the lower jaw. The union of these

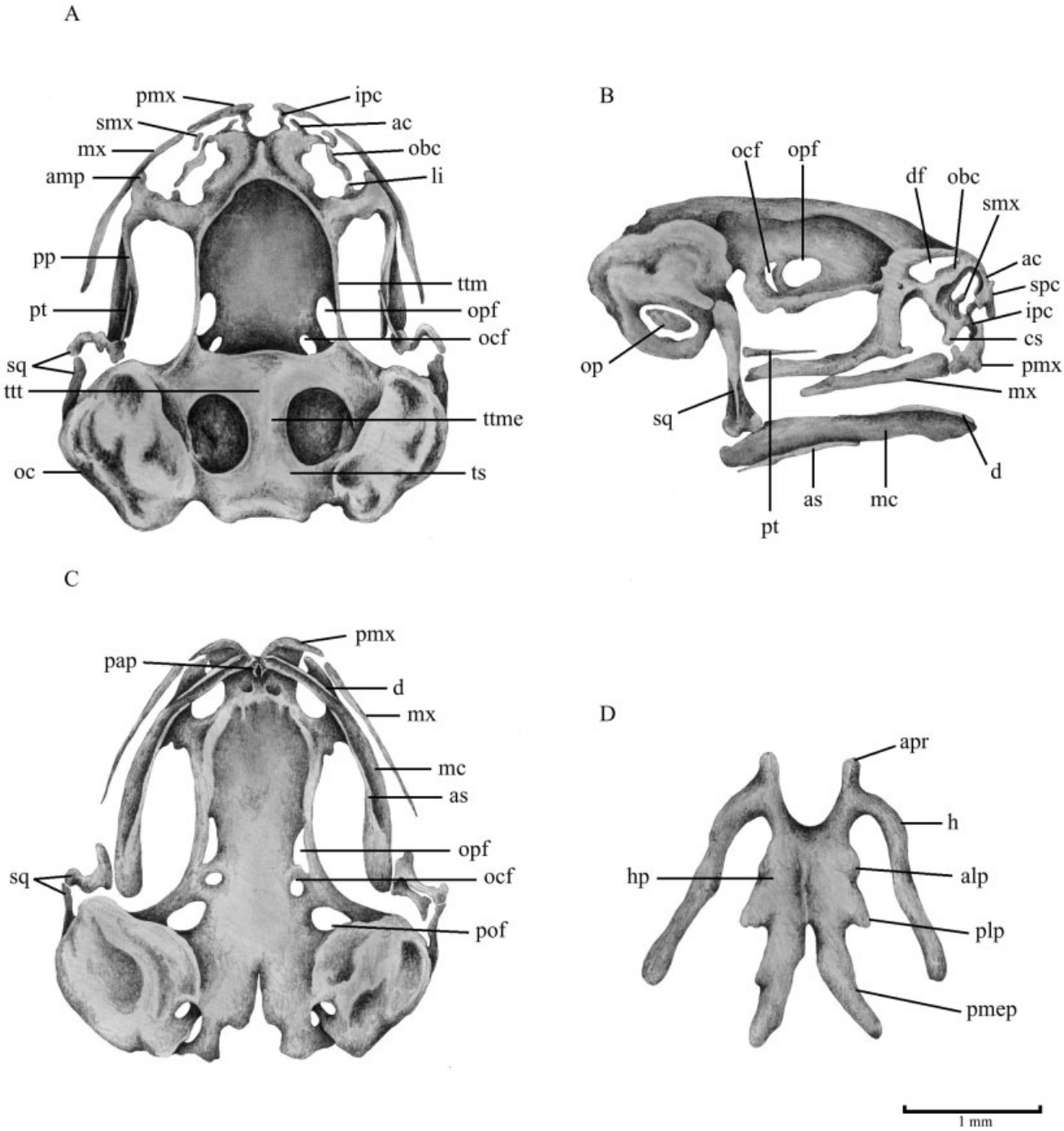


Fig. 8. *Eupsophus calcaratus* Stage 46. Skeleton. **A:** Chondrocranium, dorsal view. **B:** Chondrocranium, lateral view. **C:** Chondrocranium, ventral view. **D:** Hyobranchial skeleton, ventral view. ac, alary cartilage; alp, anterolateral process; amp, anterior maxillary process; apr, anterior process; as, angulosplenial; cs, crista subnasalis; d, dentary; df, dorsal fenestra; h, hyale; hp, hyoid plate; ipc, inferior prenasal cartilage; li, lamina inferior: mc, Meckel's cartilage; mx, maxilla; obc, oblique cartilage; oc, otic capsule; ocf, oculomotor foramen; op, operculum; opf, optic foramen; pap, palatine process; plp, posterolateral process; pmep, posteromedial process; pmx, premaxilla; pof, prootic foramen; pp, pterygoid process; pt, pterygoid; smx, septomaxilla; spc, superior prenasal cartilage; sq, squamosal; ttm, taenia tecti marginalis; ttme, taenia tecti medialis; ttt, taenia tecti transversalis; ts, tectum synoticum.

slips (*quadratoangularis* + *suspensorioangularis* + *hyoangularis* + *suspensoriohyoideus* + *orbitohyoideus*) constitutes the *M. depressor mandibulae*. Both *Mm. geniohyoideus medialis* are well developed and join in a single tendon inserted on the jaw symphysis. The *Mm. geniohyoideus lateralis* are also developed, originating on the anterior region of each hemimandible. The four muscles concur in their pos-

terior insertion, next to the base of the posterolateral processes of the hyoid plate. The *M. genioglossus* retains the configuration shown at Stage 39. The *M. hyoglossus* inserts posteriorly at the base of the posteromedial process of the hyoid plate.

Due to the profound restructuring of the hyoid, some branchial muscles lose their attachment on cartilages. The *Mm. constrictor branchialis III* and *IV*, and the *Mm. subarcualis II–IV* disappear. The *M. constrictor branchialis II* joins the *Mm. levator arcus brachialium I* and *II*, forming the *M. petrohyoideus I*. The *Mm. levator arcus branchialium III* and *IV* will constitute the *Mm. petrohyoideus II* and *III,* respectively.

### Stage 46

**External morphology.** The tail bud is completely reabsorbed. The other morphological characteristics remain invariable. Some vitellum remains in the abdomen.

**Skeleton (Fig. 8).** The cartilaginous nasal skeleton is completely configured. The maxillae, the pterygoid process, and the lower jaw lengthen, almost reaching the otic region. A slight calcification is detected in the dentaries and the anterior region of the angulosplenials. The palatoquadrate has rotated to a completely vertical position and begins to outline the basal process, a new connection with the otic capsule. Finally, the anterior primordium of the pterygoid arises as a slender sliver located dorsaly to the pterygoid process.

**Musculature (Fig. 9).** The *Mm. subarqualis rectus I* disappears and the *M. hyoglossus* enlarges, inserting near the tip of the posteromedial process of the hyoid plate.

## DISCUSSION

According to Thibaudeau and Altig (1999), nidicolous tadpoles constitute a continuum from larvae morphologically almost identical to those of exotrophic species to highly modified ones that lack several characters, such as adhesive glands, external gills, buccal apparatus, coiled intestine, lateral line system, and spiracle. The scant pigmentation during early larval stages, the great development of the hindlimbs, and the small size at metamorphosis are common traits of most nidicolous tadpoles. *Eupsophus calcaratus* tadpoles do not differ from typical exotrophic larvae in most of their external characters (oral disc, keratinized mouthparts, spiracular tube and opening). On the contrary, the scarcity of pigmentation and the development of hindlimbs (30% of the body length in Stage 31) are traits common to endotrophs. The scant pigmentation is frequently associated also with dark microhabitats, a characteristic of the *E. calcaratus* larval environment.

Among nidicolous tadpoles, the only slightly modified *Eupsophus calcaratus* tadpoles are similar to the larvae of *Cycloramphus stejnegeri* and *Colostethus chalcopis* (Heyer, 1983; Kaiser and Altig, 1994), and different from those of *Flectonotus* (no keratodonts and/or marginal papillae, and in some species reduced number of gills), *Colostethus stepheni* (no buccal apparatus), *C. nidicola* and *C. degranvillei* (reduced or absent buccal apparatus and no spiracle), *Adenomera hylaedactyla* (no spiracle), and *Syncope antenori* (no gills and highly reduced intestine) (Heyer and Silverstone, 1969; Duellman and Gray, 1983; Juncá et al., 1994; Krügel and Richter, 1995; Haas, 1996a; Caldwell and Lima, 2003).

Regarding internal morphology, published information exists for only two nidicolous species, *Cycloramphus stejnegeri* (Lavilla, 1991) and *Flectonotus goeldii* (Haas, 1996a). The three species share the nondivided supra- and infrarostral structures directly involved with the mechanism of food intake, and show, in turn, similarities with certain types of exotrophic tadpoles. Likewise, they share the general structure of the hyobranchial apparatus, with simple ceratohyals and ceratobranchials, copula I absent, and barely chondrified, reduced or absent spicules. *Eupsophus* and *Cycloramphus* also share the fusion of the pars reuniens, copula II, and hypobranchial plates and the reduction of the urobranchial process. Again, it is possible to find these traits in several exotrophic tadpoles. The reduction of spicules and the absence of lateral projections of the ceratobranchials, for instance, are supposed to be linked to macrophagous feeding (among others, Haas, 1996a; Vera Candioti et al., 2004; Vera Candioti and Haas, 2004; Vera Candioti, in press). In fact, neither macrophagous nor endotrophic larvae depend on an efficient filtering mechanism to obtain their food. The absence of copula I is frequent among anuran larvae, and cannot be related to feeding modes (but, again, the lack of copula I is a trait common to most macrophagous and endotrophic larvae).

Regarding musculature, two of the muscles generally present in other species of neobratrachians are absent in *Eupsophus calcaratus*: the *M. levator mandibulae externus superficialis* and *M. subarcualis obliquus.* The *M. l. m. e. superficialis* has a variable distribution within Leptodactylidae, and in Telmatobiinae, is absent in *Telmatobius* cf. *atacamensis* (MFVC pers. obs.). The second case is striking, because the *M. subarcualis obliquus* is present in all known species, including tadpoles without an urobranchial process, one of its attachment sites. Even in *Flectonotus goeldii*, in which the branchial musculature is reduced, with some muscles poorly developed or absent (Haas, 1996a), the *M. subarcualis obliquus* is present.

Comparison with other endotrophic, non-nidicolous larvae, for which part of the internal morphology is known, such as *Gastrotheca christiani* and

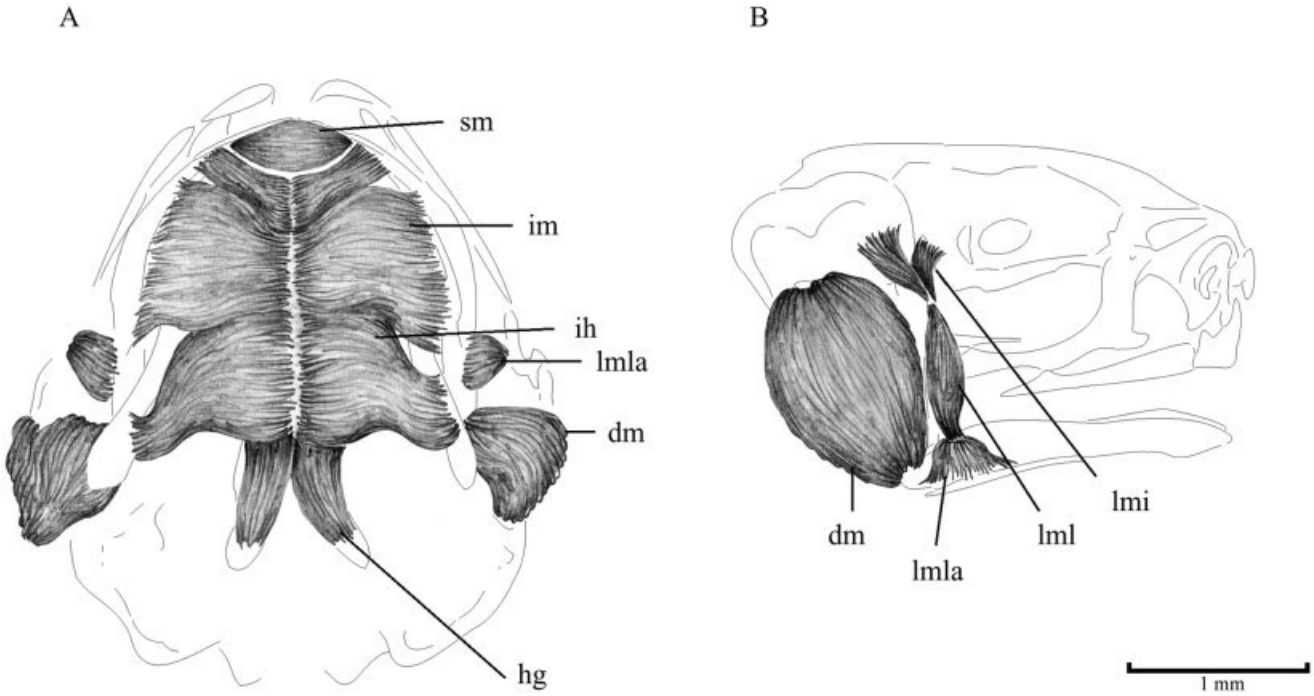


Fig. 9. *Eupsophus calcaratus* Stage 46. Musculature. **A:** Ventral view. **B:** Lateral view. dm, *depressor mandibulae*; hg, *hyoglossus*; ih, *interhyoideus*; im, *intermandibularis*; lmi, *levator mandibulae internus*; lml, *levator mandibulae longus*; lmla, *levator mandibulae lateralis*; sm, *submentalis*.

*Rhinoderma darwiniii* (Lavilla, 1987; Lavilla and Vaira, 1997) is also of interest. Although the patterns of development among these taxa differ (the free-living *Eupsophus calcaratus* larvae develop in small puddles, whereas those of *R. darwiniii* are confined to the modified vocal sac of males, and those of *G. christiani* inside a dorsal pouch in females), they show several similarities in structure. The most remarkable differences lie in the hyobranchial apparatus, surprisingly conventional in *G. christiani* and *R. darwiniii* (although the latter lacks copula I and lateral projections in the ceratobranchials, and spicules are vestigial). The absence of studies of musculature precludes any comparison in this subject.

The uniqueness of *Eupsophus calcaratus* tadpoles is a consequence of the timing of metamorphic changes. When compared to exotrophic leptodactylids (*Pleurodema borelli*—Fabrezi, 1988; *Ceratophrys cornuta*—Wild, 1997; *Chacophrys pierotii*—Wild, 1999), the changes in the *E. calcaratus* chondrocranium and visceral skeleton are delayed. Thus, at the end of metamorphosis the cephalic skeleton of *E. calcaratus* retains some larval traits, such as minimal calcification, persisting parietal fenestrae, and the adult otic process still not differentiated. In the particular case of the nidicolous larvae, the only possible comparison is with *Flectonotus goeldii* (Haas, 1996a). In Stage 38–39, the ethmoid region of *Flectonotus* has more advanced development that in *E. calcaratus*, but the parietal fenestrae also persist postmetamorphically.

Regarding ossification sequence, Trueb (1985) reviewed 18 species from eight families and pointed out that in most anurans frontoparietals, exoccipitals, and parasphenoid ossify before the onset of the metamorphosis, whereas septomaxillae, premaxillae, maxillae, dentaries, angulosplenials, squamosals, nasals, prootics, mentomeckelians, quadratojugals, palatines, pterygoids, and vomers mineralize at metamorphic climax, and the sphenethmoid, columella, and neomorphic elements ossify postmetamorphically. Later studies on other species coincide in general with Trueb's summary (i.e., *Hyla lanciformis*—De Sá, 1988; *Pleurodema borelli*—Fabrezi, 1988; *Spea bombifrons*—Wiens, 1989; *Xenopus laevis*—Trueb and Hanken, 1992; *Gastrotheca riobambae*—Haas, 1996b; *Discoglossus sardus*—Púgener and Maglia, 1997; *Ceratophrys cornuta*—Wild, 1997; *Pyxicephalus adspersus*—Sheil, 1999; *Chacophrys pierotti*—Wild, 1999; *Leptodactylus chaquensis*—Perotti, 2001). In *Eupsophus calcaratus* the sequence diverges from the general pattern, both in the stages at which ossifications appear and in the general order of appearance. The first primordia are those of the maxillary arch, upper and lower jaw, and suspensorium; the pterygoids form toward the end of metamorphosis, as in most anurans. All the remaining elements differentiate and ossify postmetamorphically, including those elements that

*TABLE 3. Comparison of ossification sequence in nidicolous and most of anuran larvae*

| | General sequence* (Trueb, 1985) | *Eupsophus calcaratus* (present study) | *Flectonotus goeldii* (Haas, 1996a) |
|---|---|---|---|
| | parasphenoid<br>frontoparietals<br>exoccipitals | | frontoparietals<br>parasphenoid |
| METAMORPHOSIS ONSET<br>(Stage 41) | | | |
| Early Metamorphosis | septomaxillae<br>premaxillae<br>maxillae<br>dentaries<br>angulosplenials<br>squamosals<br>nasals<br>prootics<br>mentomeckelians | septomaxillae<br>premaxillae<br>maxillae<br>dentaries<br>angulosplenials<br>squamosals<br>pterygoids | Not specified |
| Late Metamorphosis | quadratojugals<br>palatines<br>pterygoids<br>vomers | | |
| (Stage 46)<br>METAMORPHOSIS TERMINATION | | | |
| | columella<br>sphenethmoid<br>neomorphic elements | columella*<br>sphenethmoid<br>exoccipitals<br>frontoparietals<br>mentomeckelians<br>neomorphic elements<br>palatines<br>parasphenoid<br>quadratojugals<br>vomers | |

*The order in which ossification is listed within each period is not necessarily exact.

in most anurans are the first to appear, i.e., frontoparietals, parasphenoid, and exoccipitals. Significant deviations from the general pattern are verified in a minority of species. In *Osteopilus septentrionalis,* frontoparietals and septomaxillae ossify at Stage 45 (although delayed, they are still the first to appear), and all the remaining structures arise postmetamorphically (Trueb, 1966). In *Pseudacris triseriata* the parasphenoid ossifies not only postmetamorphically but also later than most of the other bones (Stokely and List, 1954). Changes in the general order of the sequence appear too in *Hamptophryne boliviana, Triprion petasatus*, and *Bombina orientalis*, where the bones of suspensorium and mandible ossify postmetamorphically (Trueb, 1970; De Sá and Trueb, 1991; Maglia and Púgener, 1998). Among nidicolous tadpoles, *Flectonotus goeldii* has frontoparietals and septomaxillae ossified at Stage 38–39, like most anurans (Haas, 1996a; the appearance of the remaining structures is not detailed in the article). The absence of studies on other nidicolous larvae does not allow further conclusions on this subject. Table 3 shows the ossification sequence for most anurans, *E. calcaratus*, and *F. goeldii*, following the scheme presented by Trueb (1985).

The studies regarding muscle metamorphosis are even fewer, and unavailable for nidicolous larvae. Taking as a reference the works by Starrett (1968) and Fabrezi (1988), our results coincide with what was described for *Pleurodema borellii*, characterized by the absence of *M. levator mandibulae externus superficialis* in tadpoles and adults, and the double origin of the *M. depressor mandibulae.*

To conclude, *Eupsophus calcaratus* larvae are located near one of the extremes of the continuum proposed by Thibaudeau and Altig (1999), with a mixture of external characters similar to those of exotrophic tadpoles and a few typical of endotrophs. Despite the existence of some peculiarities, the endotroph-nidicolous developmental mode lacks any exclusive character state in the structure of the neurocranium and hyobranchial apparatus. *Eupsophus calcaratus* tadpoles show particular heterochronic traits, with delayed development of several structures, with regard to most of the anurans described (e.g., restructuring of the ethmoid region, palatoquadrate, and hyobranchial skeleton), and structures that keep their larval condition after the end of larval life (e.g., persisting parietal fenestrae, absence of adult otic process and several bones). Like other nonfeeding larvae (Krügel and Richter, 1995), the development of *E. calcaratus* seems to be relatively fast, as a consequence of the limited vitellum supply. Indeed, most of the modifications in skeleton and musculature occur rapidly in early Stage 43. According to Haas (1996a), a truncated larval development corresponds to a short larval

life and a smaller size at metamorphosis. Effectively, *E. calcaratus* tadpoles (and other congeneric species, Díaz and Valencia, 1985) metamorphose in 8–9 weeks and have a size at metamorphosis less than 1.2 cm.

Endotrophic tadpoles are a really interesting and still poorly explored field. Future studies providing baseline data that tend to complete the gaps in our knowledge will be very useful to understand variation in morphology, developmental patterns, and phylogenetic relationships among anuran larvae.

## ACKNOWLEDGMENT

We thank the two anonymous reviewers for greatly improved an earlier version of this article.

## LITERATURE CITED

Altig R, Johnston GF. 1989. Guilds of anuran larvae: relationships among developmental modes, morphologies and habits. Herpetol Monogr 2:81–109.

Bock JW, Shear CR. 1972. A staining method for gross dissection of vertebrate muscles. Anatomischer Anzeiger 130:222–227.

Caldwell JP, Lima AP. 2003. A new species of *Colostethus* (Anura: Dendrobatidae) with a nidicolous tadpole. Herpetologica 59: 219–234.

Canatella D. 1999. Architecture. Cranial and axial musculoskeleton. In: McDiarmid RW, Altig R, editors. Tadpoles. The biology of anuran larvae. Chicago: University of Chicago Press. p 52–91.

De Sá RO. 1988. Chondrocranium and ossification sequence of *Hyla lanciformis.* J Morphol 195:345–355.

De Sá RO, Trueb L. 1991. Osteology, skeletal development, and chondrocranial structure of *Hamptophryne boliviana* (Anura: Microhylidae). J Morphol 209:311–330.

Díaz NF, Valencia J. 1985. Larval morphology and phenetic relationships of the Chilean *Alsodes, Telmatobius, Caudiverbera* and *Insuetophrynus* (Anura: Leptodactylidae). Copeia 1985: 175–181.

Duellman WE, Gray P. 1983. Developmental biology and systematics of the egg-brooding hylid frogs, genera *Flectonotus* and *Fritziana.* Herpetologica 39:333–359.

Fabrezi M. 1988. Metamorfosis en *Pleurodema borellii* (Anura: Leptodactylidae). Estudio del neurocráneo, esqueleto visceral y musculatura asociada. Unpublished Thesis. Universidad Nacional de Tucumán, Tucumán, Argentina.

Formas RJ. 1989. The tadpole of *Eupsophus calcaratus* in southern Chile. J Herpetol 23:195–197.

Gosner KL. 1960. A simplified table for staging anuran embryos and larvae, with notes on identification. Herpetologica 16:183–190.

Haas A. 1996a. Nonfeeding and feeding tadpoles of hemiphractinae frogs: larval head morphology, heterochrony and systematics of *Flectonotus goeldii* (Amphibia, Anura, Hylidae). J Zool Syst Evol Res 34:163–171.

Haas A. 1996b. Das larvale Cranium von *Gastrotheca riobambae* und seine Metamorphose (Amphibia, Anura, Hylidae). Verh Naturwiss Ver Hamburg 36:33–162.

Heyer R. 1983. Notes on the frog genus *Cycloramphus* (Amphibia: Leptodactylidae), with descriptions on two new species. Proc Biol Soc Washington 96:548–559.

Heyer R, Silverstone PA. 1969. The larva of the frog *Leptodactylus hylaedactylus* (Leptodactylidae). Field Zool 51:141–145.

Juncá FA, Altig R, Gascon C. 1994. Breeding biology of *Colostethus stepheni*, a dendrobatid frog with a nontransported nidicolous tadpole. Copeia 1994:747–750.

Kaiser H, Altig R. 1994. The atypical tadpole of the dendrobatid frog, *Colostethus chalcopis*, from Martinique, French Antilles. J Herpetol 28:374–378.

Krügel P, Richter S. 1995. *Syncope antenori* — a bromeliad breeding frog with free-swimming, non-feeding tadpoles (Anuran: Microhylidae). Copeia 1995:955–963.

Lavilla EO. 1987. La larva de *Rhinoderma darwinii* D & B (Anura: Rhinodermatidae). Acta Zool Lilloana 39:81–88.

Lavilla EO. 1991. Condrocráneo y esqueleto visceral en larvas de *Cycloramphus stejnegeri* (Leptodactylidae). Amphibia-Reptilia 12:33–38.

Lavilla EO, Vaira M. 1997. Larval chondrocranium of *Gastrotheca christiani* (Hylidae), with comments on the chondrocrania of non-feeding larvae in Anura. Zbynek Roček and Scott Hart: Abstracts of the Third World Congress of Herpetology. Prague, Czech Republic. p 124.

Maglia AM, Púgener LA. 1998. Skeletal development and adult osteology of *Bombina orientalis* (Anura: Bombinatoridae). Herpetologica 54:344–363.

Perotti MG. 2001. Skeletal development of *Leptodactylus chaquensis* (Anura: Leptodactylidae). Herpetologica 57:318–335.

Púgener LA, Maglia AM. 1997. Osteology and skeletal development of *Discoglossus sardus* (Anura: Discoglossidae). J Morphol 233:267–286.

Sheil CA. 1999. Osteology and skeletal development of *Pyxicephalus adspersus* (Anura: Ranidae: Raninae). J Morphol 240:49–75.

Starrett P. 1968. The phylogenetic significance of the jaw musculature in anuran amphibians. PhD Thesis. Ann Arbor: University of Michigan.

Stokely PS, List JC. 1954. The progress of ossification in the skull of the cricket frog *Pseudacris nigrita triseriata.* Copeia 1954: 211–217.

Thibaudeau G, Altig R. 1999. Endotrophic anurans. In: McDiarmid RW, Altig R, editors. Tadpoles. The biology of anuran larvae. Chicago: University of Chicago Press. p 170–188.

Trueb L. 1966. Morphology and development of the skull in the frog *Hyla septentrionalis.* Copeia 1966:562–573.

Trueb L. 1970. Evolutionary relationships of casque-headed treefrogs with co-ossified skulls. Univ Kansas Publ Mus Nat Hist 18:547–716.

Trueb L. 1985. A summary of osteocranial development in anurans with notes on the sequence of cranial ossification in *Rhinophrynus dorsalis* (Anura: Pipoidea: Rhinophrynidae). S Afr J Sci 81:181–185.

Trueb L, Hanken J. 1992. Skeletal development in *Xenopus laevis* (Anura: Pipidae). J Morphol 214:1–41.

Vera Candioti MF. In press. Morphology and feeding in tadpoles of *Ceratophrys cranwelli* (Anura: Leptodactylidae). Acta Zool.

Vera Candioti MF, Haas A. 2004. Three dimensional reconstruction of the hyobranchial apparatus of *Hyla nana* tadpoles (Anura: Hylidae). Cuad Herpetol 18:3–15.

Vera Candioti MF, Lavilla EO, Echeverría DD. 2004. Feeding mechanisms in two treefrogs, *Hyla nana* and *Scinax nasicus* (Anura: Hylidae). J Morphol 261:206–224.

Wassersug RJ. 1976. A procedure for differential staining of cartilage and bone in whole formalin-fixed vertebrates. Stain Technol 51:131–134.

Wiens JJ. 1989. Ontogeny of the skeleton of *Spea bombifrons* (Anura: Pelobatidae). J Morphol 202:29–51.

Wild ER. 1997. Description of the adult skeleton and developmental osteology of the hyperossified horned frog, *Ceratophrys cornuta* (Anura: Leptodactylidae). J Morphol 232:169–206.

Wild ER. 1999. Description of the chondrocranium and osteogenesis of the Chacoan burrowing frog, *Chacophrys pierotti* (Anura: Leptodactylidae). J Morphol 242:229–246.

*APPENDIX*
Eupsophus calcaratus *specimens examined*

a. External morphology

| | | |
|---|---|---|
| Stage 31.1 specimen | Stage 36.6 specimens | Stage 42.4 specimens |
| Stage 31–32.1 specimen | Stage 37.5 specimens | Stage 43.1 specimen |
| Stage 33.1 specimen | Stage 37–38.1 specimen | Stage 44.5 specimens |
| Stage 34.1 specimen | Stage 38.5 specimens | Stage 45.1 specimen |
| Stage 34–35.1 specimen | Stage 41.4 specimens | |
| Stage 35.5 specimens | Stage 41–42.1 specimen | |

b. Internal morphology

| | | |
|---|---|---|
| Stage 31.1 specimen | Stage 38.1 specimen | Stage 43–44.1 specimen |
| Stage 33–34.3 specimens | Stage 39.1 specimen | Stage 44.1 specimen |
| Stage 36.1 specimen | Stage 42.2 specimens | Stage 46.1 specimen |